Talanta 232 (2021) 122417

Contents lists available at ScienceDirect

Talanta

journal homepage: www.elsevier.com/locate/talanta

A malachite green light-up aptasensor for the detection of theophylline

Arghya Sett [a,1], Lorena Zara [a,1,2], Eric Dausse [a], Jean-Jacques Toulmé [a,b,*]

[a] Univ Bordeaux, CNRS, Inserm, ARNA, UMR5320, U1212, F-33000, Bordeaux, France
[b] Novaptech, F-33600, Pessac, France

ARTICLE INFO

Keywords:
Aptamer
Malachite green
Fluorescence
RNA hairpin
Kissing complex
Biosensor

ABSTRACT

Biosensors are of interest for the quantitative detection of small molecules (metabolites, drugs and contaminants for instance). To this end, fluorescence is a widely used technique that is easily associated to aptamers. Light-up aptamers constitute a particular class of oligonucleotides that, specifically induce fluorescence emission when binding to cognate fluorogenic ligands such as malachite green (MG). We engineered a dual aptasensor for theophylline (Th) based on the combination of switching hairpin aptamers specific for MG on the one hand and for Th on the other hand, hence their names: malaswitch (Msw) and theoswitch (Thsw). The two aptaswitches form a loop-loop or kissing Msw-Thsw complex only in the presence of theophylline, allowing binding of MG, subsequently generating a fluorescent signal. The combination of the best Msw and Thsw variants, MswG12 and Thsw19.1, results in a 20-fold fluorescence enhancement of MG at saturating theophylline concentration. This aptasensor discriminates between theophylline and its analogues caffeine and theobromine. Kissing aptaswitches derived from light-up aptamers constitute a novel sensing device.

1. Introduction

Since the onset of aptamers, scientists are exploring the application of these oligonucleotides as sensor modules for diagnostic and various analytical applications [1–5]. Over the last decade, RNA aptamers were developed which induce fluorescence enhancement after binding to their cognate fluorogen molecule [6–11]. Such "light up" aptamers are promising tools for monitoring cellular functions and for tracking metabolites in cultured cells [12–17]. Light-up aptamers actually constitute an alternative to fluorescent reporter proteins (GFP, YFP etc.) of special interest for detecting RNA species [7,18].

Generally, light up RNA aptamers for organic flurophores like DFHBI, malachite green and thiazole orange possess some structural flexibility. Structural studies of these RNA aptamers showed that many fluorogenic dyes interact with parallel/antiparallel G-quadruplexes although the structure of flanking regions also influences the fluorescence emission [10,19,20]. Jaffrey and coworkers developed a sensor-based riboswitch by integrating SAM, GTP or ADP aptamers in the 'stem' sequence of the Spinach light-up aptamer [7].

Malachite green (MG) is an organic tri-phenyl methane dye with a quantum yield of 7.9×10^{-5} *i.e.* almost non-fluorescent when alone in aqueous solution [21]. An RNA aptamer for malachite green was discovered that induces more than 2000 fold fluorescence increase upon binding to the dye [6,21,22]. In contrast to DFHBI or thiazole orange light-up aptamers, the MG aptamer folds into an imperfect hairpin. Structural insights of malachite green aptamer identified the nucleotides and the MG groups involved in the interaction between the dye and the oligonucleotide [21,23].

We took advantage of this hairpin structure for engineering a new type of aptasensor. We previously demonstrated that the formation of loop-loop RNA complexes (so-called "kissing" complexes) can be exploited for sensing different ligands [18,24–27]. We recently converted the malachite green RNA aptamer into a switching aptamer (we called it an aptaswitch). In response to kissing interactions, the aptamer switches between an open (unfolded) and a closed (folded) structure. Only the folded one binds the dye, thus allowing the specific detection of hairpin precursors of microRNAs by fluorescence [18,28].

In the present study we used a similar strategy for engineering malachite green-based fluorescent sensors for the detection of a small molecule: theophylline. To this end two modules specific for malachite green that will generate the signal on the one hand and for the target ligand theophylline on the other hand should be designed, that will

* Corresponding author. Univ Bordeaux, CNRS, Inserm, ARNA, UMR5320, U1212, F-33000, Bordeaux, France.
E-mail address: jean-jacques.toulme@inserm.fr (J.-J. Toulmé).
[1] These authors contributed equally to the work.
[2] Present Address: Novaptech, F-33600, Pessac, France.

https://doi.org/10.1016/j.talanta.2021.122417
Received 3 December 2020; Received in revised form 1 April 2021; Accepted 8 April 2021
Available online 20 April 2021

interact through kissing interactions depending on the simultaneous presence of the two cognate ligands.

The theophylline RNA aptamer, first isolated by Jenison and co-workers in 1994, was so specific toward its target that it could differentiate the chemical analogue caffeine which is a methyl derivative of theophylline [29]. Since then, this RNA hairpin aptamer was widely used in cellular engineering, synthetic biology and other diagnostic applications [30,31]. We converted the malachite green and the theophylline hairpin aptamers into aptaswitches (malaswitch Msw and theoswitch Thsw, respectively) by modifying the apical part of the parent oligomers that is not involved in the recognition of their targets. First a kissing prone sequence was substituted to their apical loop. Second the double-stranded connector between this loop and the target-binding site (a central loop) was shortened in such a way that the modified aptamers do no longer bind their target. The affinity for the dye or for theophylline is restored by loop-loop interaction, likely through stacking interaction between the loop-loop nucleic acid base pairs and the aromatic moiety of the target molecules. We report here the engineering of such a kissing biosensor that quantitatively and specifically translates the recognition of theophylline into malachite green fluorescence.

2. Materials and methods

2.1. Oligonucleotides and chemicals

Synthetic oligodeoxynucleotides purified by polyacrylamide gel electrophoresis were purchased from Eurogentec. The concentration of oligonucleotide solutions was measured on a Nanodrop spectrophotometer. Theophylline, caffeine, theobromine, malachite green and other chemicals (HEPES buffer, sodium acetate, potassium acetate, magnesium acetate) were purchased from Sigma-Aldrich.

2.2. In vitro transcription

RNA aptaswitch candidates were in-vitro transcribed by T7-Flashscribe™ transcription kit (Cellscript). In a standard 20 µl reaction volume, 1 µg of DNA templates containing the complementary sequence of the T7 promoter (5′ TAATACGACTCACTATAG 3 ‘) at the 3’ end of the template were transcribed with ATP, UTP, GTP and CTP (100 mM of each), 100 mM DTT (2 µl), Type I RNase Inhibitor (0.5 µl), T7 reaction buffer (10x) and 2 U of T7 RNA polymerase. The reaction mixture was kept at 37 °C for 2 h followed by DNAse (1U) treatment for 20 min. Gel purified RNA transcripts were verified by electrophoresis on a 20% denaturing polyacrylamide gel and stored at −20 °C in water for further use.

2.3. Fluorescence measurements

Malaswitch variants were heated for 2 min at 65 °C and then kept on ice for 5 min. SE 5x buffer was added to the mixture and incubated at room temperature for 15 min (SE x1 buffer contains 20 mM HEPES pH 7.4, 20 mM sodium acetate, 140 mM potassium acetate and 3 mM magnesium acetate). Deionized water was added to adjust the required concentration of the aptaswitch candidates. Following the folding of malaswitches, malachite green was added. In parallel, RNA hairpin K3 alone or theoswitch variants in the presence of theophylline (or caffeine, or theobromine) were also folded according to the protocol described above. Malaswitch-K3 or malaswitch-theoswitch mixtures were incubated for 2 h at 4 °C in the dark in the presence of their cognate ligands. Fluorescence measurements of 50 µl samples were then performed in triplicate. Background signal was subtracted to fluorescence signals.

The fluorescence properties of theoswitch variants were tested in the presence or in the absence of theophylline. 4 µM of theoswitch variants in SE buffer were folded with or without 8 mM of theophylline and 0.1 µM malaswitch was folded with 1 µM of malachite green. All fluorescence measurements were performed at 650 nm in triplicate on a Tecan Infinite M100 spectrofluorimeter, following excitation at 610 nm.

3. Results and discussion

3.1. Rationale engineering of an aptaswitch for malachite green (malaswitch Msw)

We converted the malachite green specific RNA aptamer into a structure-switching aptaswitch (we name it ‘malaswitch’) [6]. We used the same rationale as the one previously employed for generating malaswitches able to sense precursors of microRNAs [18] (Scheme 1). The original apical loop of the malachite green aptamer that is not involved in the recognition of the dye was substituted by a sequence prone to loop-loop interaction with the small RNA hairpin K3: 5′CGAGCCUGGGAGCUCG3’ (Fig. 1).

We investigated the binding behaviour of 4 variants in which the motif 5′-XCCCAG-3’ (X = C,G,U), complementary to part of the K3 loop (underlined in the K3 sequence above), was introduced. In addition we destabilized the top part of the aptamer in such a way that it cannot any longer bind the malachite green alone [25]. To this end, the connector between the apical loop and the internal loop corresponding to the dye binding site was restricted to 2 base pairs, (UA and CG). The 4 variants MswK3′, MswG12A20, MswC12 and MswG12 are shown on Fig. S1 and their sequence is given in Table S1.

Compared to the parent aptamers all 4 variants induced a very poor fluorescence emission of the dye (Fig. 2) likely due to the destabilisation of the top part of the aptamer that does not provide a sufficient contribution to the formation of the dye-RNA complex. This is indeed what we expected from our design.

We then evaluated the effect of K3 on the malachite green-aptamer interaction. All 4 variants responded to the simultaneous addition of the dye and of K3 by a fluorescence enhancement. Upon addition of 2 µM of K3 to a mixture of 0.1 µM of the different malaswitch variants with 2 µM of malachite green the fluorescence was increased 12, 18 and 10 fold for MswK3′, MswG12A20 and MswC12, respectively, compared to the emission of the dye in the absence of K3 (Fig. 2). The largest enhancement (50 fold) was observed with MswG12 that displayed under these conditions a fluorescence signal even higher than the parent aptamer (Fig. 2). This is very likely related to the stabilisation of the aptamer-malachite green complex by the kissing interaction. Indeed no such an increase was observed when K3Mut was substituted to K3 in the ternary mixture (Fig. 2). The loop sequence of K3Mut 5′CUG**AC**GA (Fig. 1) did not allow the formation of a loop-loop helix with MswG12 due to the presence of two point mutations (in bold in the K3Mut sequence).

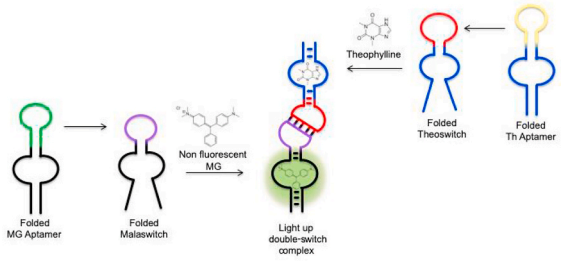

Scheme 1. Design of the malaswitch-theoswitch fluorescent sensor. The apical parts of the parent malachite green MG and theophylline aptamers (purple and red lines, respectively) were changed in such a way to promote the formation of a loop-loop complex. The loop complementary to K3 (see Fig. 1) was substituted to the original apical loop of the MG aptamer whereas the loop K3 was incorporated in the top part of the theophylline aptamer so that the resulting malaswitch (Msw) can form a stable kissing complex either with K3 in the presence of the fluorogen malachite green MG or with the theoswitch in the presence of both theophylline and MG, hence generating a fluorescence signal.

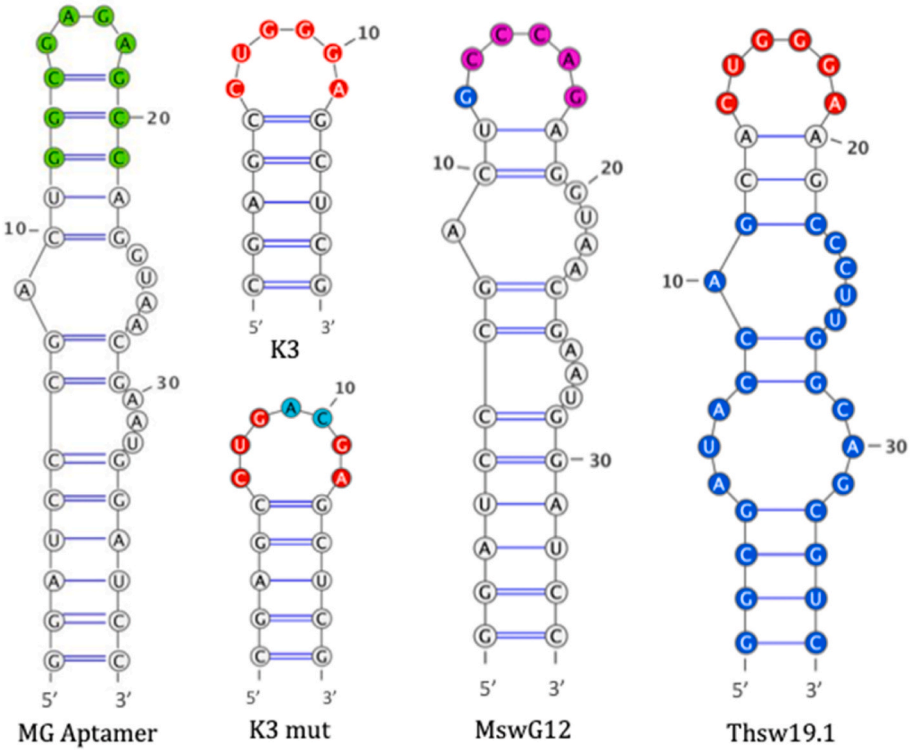

Fig. 1. Secondary structures of Malachite green aptamer, malaswitch and theoswitch. Predicted secondary structure of the malachite green (MG) aptamer [21] and sequences of the malaswitch MswG12 and of the theoswitch Thsw19.1. The hairpins K3 and K3Mut are also shown. The complementary bases susceptible to generate a loop-loop helix are highlighted in pink for MswG12 and in red (K3 and theoswitch 19.1). The mutations are indicated in cyan for K3Mut. (For interpretation of the references to colour in this figure legend, the reader is referred to the Web version of this article.)

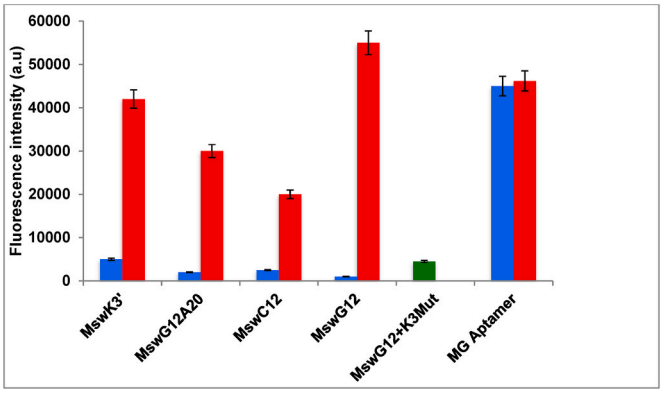

Fig. 2. Fluorescence properties of Malaswitches. Fluorescence of malachite green with the MG aptamer or with malaswitch variants in the absence (blue bars) or in the presence of either K3 (red bars) or K3Mut (green bar). Measurements (λ_{Exc} = 610 nm, λ_{Em} = 650 nm) were performed in triplicate at room temperature in the SE buffer containing 3 mM magnesium. (For interpretation of the references to colour in this figure legend, the reader is referred to the Web version of this article.)

3.2. *Engineering an aptaswitch for theophylline (theoswitch Thsw)*

In order to sense the presence of theophylline through MG signalling we substituted a specific aptaswitch to the hairpin K3. The idea was to convert the theophylline aptamer into a theoswitch *i.e.* an aptaswitch responding to theophylline [32,33]. The parent theophylline RNA aptamer that is an imperfect hairpin should be engineered in such a way that it forms a kissing interaction with the malaswitch described above in the presence, and only in the presence of both theophylline and malachite green. The kissing association of the theoswitch and of the malaswitch in a medium containing malachite green will result in a theophylline-dependent fluorescence emission (Scheme 1). To this end the top part of the theophylline aptamer was modified: the K3 kissing motif 5′CUGGGA3′ complementary to the MswG12 loop was introduced into the apical loop and the connector domain between the loop and the theophylline binding site was destabilized.

We rationally engineered 20 theoswitch (Thsw) variants with various purine/pyrimidine combinations in the apical loop and different lengths of the connector domain (Table S2 and Fig. S2). The sensing response of all Thsw variants was carried out by fluorescence assay at a single malachite green concentration (1 μM) in the absence and in the presence of the target molecule theophylline at saturating concentration (8 mM). Under these conditions theoswitches 17.1, 17.3, 18.3, 19.7, 19.9, 19.11, and 19.12 did not show any significant fluorescence emission meaning that either the theophylline-binding site was affected by the modification of the aptamer or that the kissing interaction could not stabilize the complex (Fig. 3). Some Thsw candidates (18.1, 19.2, 19.4 and 19.10) exhibited a strong fluorescence signal in the presence as well as in the absence of theophylline (Fig. 3) indicating that the formation of the Thsw-Msw complex was sufficient to promote the binding of the dye even without theophylline leading to a non-specific signal. Therefore, these variants cannot be exploited for bio-sensing applications. Other Thsw variants (17.2, 17.5, 18.2, 19.1, 19.3, 19.5, 19.6, 19.8) showed a theophylline-dependent fluorescence. For the variant Thsw19.1 the enhancement reached almost 20 fold, *i.e.* the MG fluorescence emission was 20 fold higher in the presence of theophylline than in its absence for the MswG12-Thsw19.1 combination.

The Thsw connector between the apical loop and the target molecule binding site and the base-base combination closing the apical loop plays a critical role in the formation of the kissing complex as previously demonstrated [34–36]. The Thsw19.1 connector consists of 2 base pairs (GC, CG) and shows a purine-purine (A-A) combination for closing the loop (Fig. S2). Purine-purine combinations were previously demonstrated to favour kissing complex formation, likely due to a larger aromatic area for stacking interaction and an extended distance between phosphate residues of the two sugar-phosphate chains, thus weakening the electrostatic repulsion [27,36,37]. However this is not a sufficient condition for ensuring specific sensing as Thsw18.1, 18.3, 19.10 and 19.12 also display a purine-purine combination but exhibit poor or

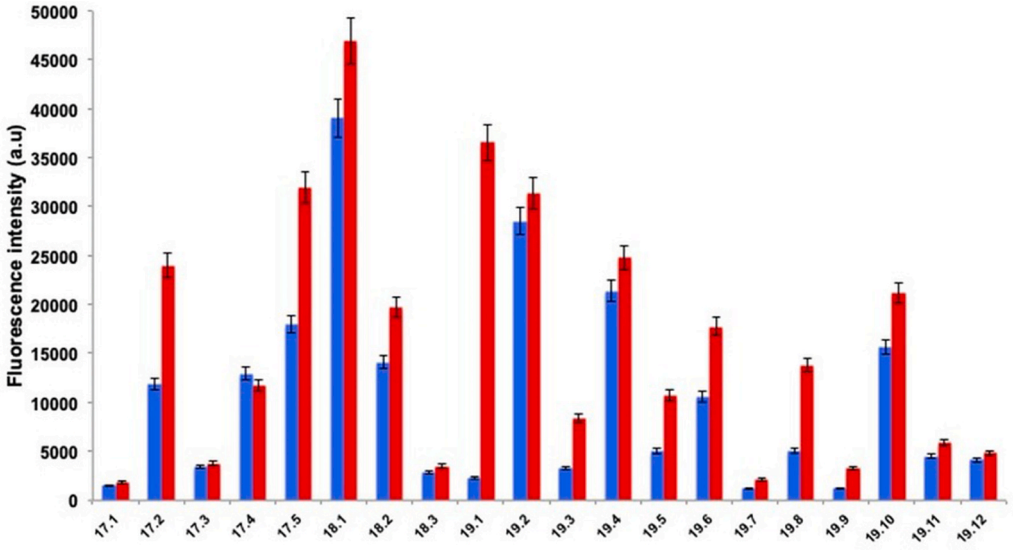

Fig. 3. Fluorescence of malachite green for different MswG12-theoswitch variants. Fluorescence emission (λ_{Exc} = 610 nm, λ_{Em} = 650 nm) of 1 μM MG in the absence (blue bars) or in the presence (red bars) of theophylline (8 mM). Measurements were performed in triplicate at room temperature in SE buffer containing 3 mM magnesium. (For interpretation of the references to colour in this figure legend, the reader is referred to the Web version of this article.)

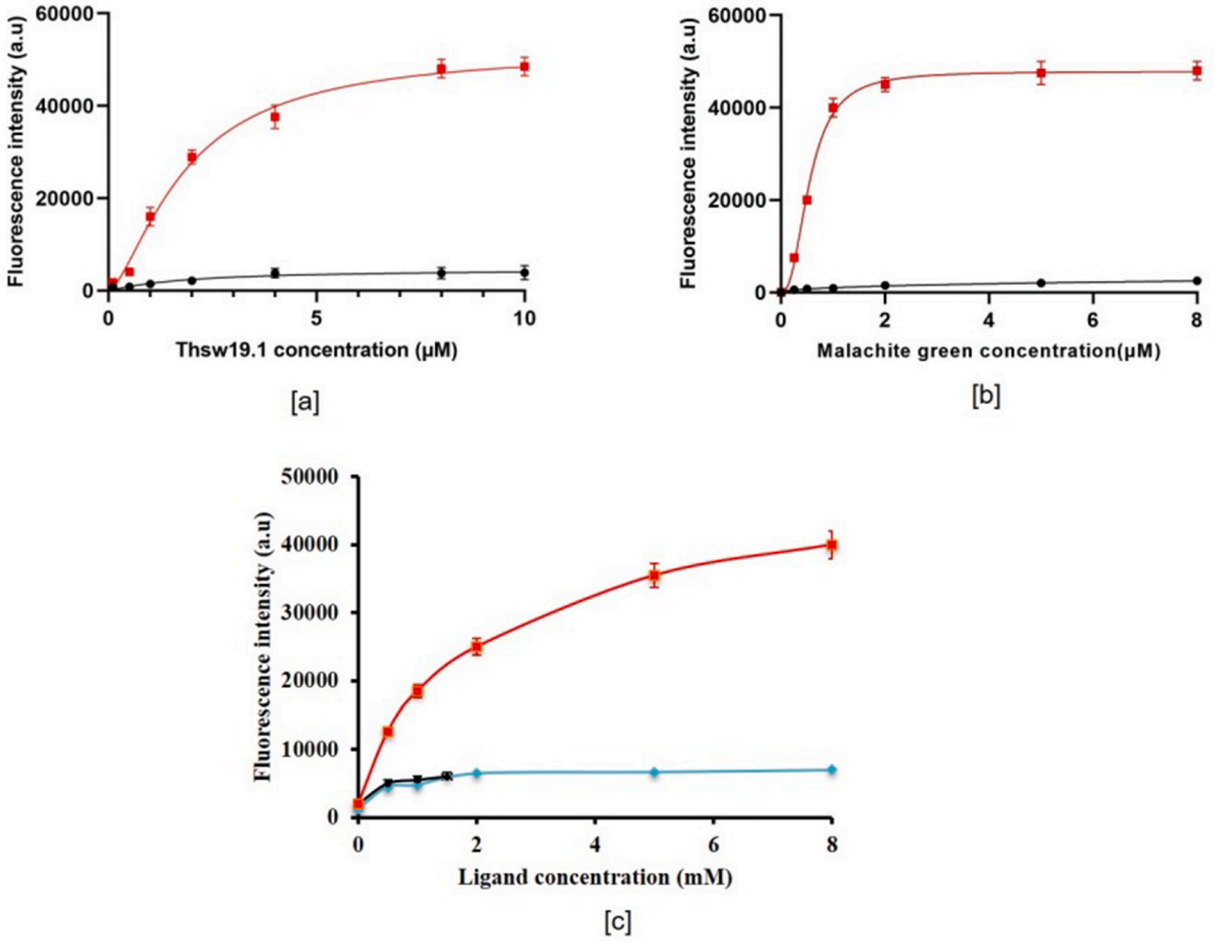

Fig. 4. Fluorescence saturation assays. a) Titration of a MswG12 (0.1 μM)- MG (1 μM) mixture by the theoswitch 19.1 in the absence (black line) and presence (red line) of theophylline 8 mM. b) MG saturation assay: Titration of a Thsw19.1 (0.1 μM)-MswG12 (4 μM) complex by malachite green in the presence (red line) and absence (black line) of theophylline. c) Fluorimetric titration of a MG (1 μM), MswG12 (0.1 μM), Thsw19.1 (4 μM) mixture by theophylline (red line), caffeine (blue line) and theobromine (black line). Fluorescence measurements (λ_{Exc} = 610 nm, λ_{Em} = 650 nm) were performed in triplicate at room temperature in SE buffer containing 3 mM magnesium. (For interpretation of the references to colour in this figure legend, the reader is referred to the Web version of this article.)

non-specific fluorescence signal. In contrast to Thsw19.1 all these variants have only one base pair in the connector.

3.3. Characterization of the malaswitch-theoswitch sensor for theophylline

We characterized the binding properties of Thsw19.1 which is the best theophylline sensing variant with respect to signal intensity. Under the conditions used for the saturation assay (0.1 μM MswG12, 1 μM malachite green and 8 mM theophylline), the plateau was reached in the low micromolar range of Thsw19.1 (Fig. 4a). As expected, only a very weak fluorescence signal was observed on the 0–10 μM concentration range in the absence of theophylline indicating the simultaneous requirement of both Msw and Thsw ligands for complex formation.

Then we performed the titration of fixed amounts of Thsw19.1 (4 μM), MswG12 (0.1 μM) and theophylline (4 mM) by malachite green. Under these conditions half saturation was obtained below 1 μM (Fig. 4b). Once again almost no fluorescence was detected in the absence of theophylline.

Last, we proceeded to the detection assay of theophylline with our sensor (Fig. 4c). The MG fluorescence signal increased with the theophylline concentration. Under our conditions half-saturation was observed around 1 mM theophylline. As shown on Fig. 4c the Thsw19.1-MswG12 combination does not respond to the addition of either caffeine or theobromine, compounds whose molecular structure is close to that of theophylline and that are not recognized by the theophylline parent aptamer. The aptaswitch variant therefore retains the characteristics of the parent aptamer: our biosensor is a stronger ligand of theophylline compared to caffeine and theobromine that differ by methyl substitutions on the purine ring.

Incidentally, the poor solubility of theobromine in water requested the addition of ethanol for preparing the stock solution used for the assay described above. Under this condition the Msw-Thsw sensor remained functional (Fig. S3). We actually demonstrated that a kissing sensor for adenosine was still able to detect the ligand up to 40% ethanol (unpublished result). Such a property is of wide interest for the detection of ligands poorly soluble in water.

4. Conclusion

In conclusion, we have designed a malachite green light-up sensor for theophylline. This was achieved by engineering two aptaswitches from the parent MG and theophylline RNA aptamers the top parts of which were modified for allowing ligand-dependent kissing interaction. Our approach led to the development of a label-free, simple sensor to detect a small size ligand. In earlier studies, several teams developed label-free MG-based sensors to detect adenosine [38,39]. They engineered the malachite green aptamer by introducing the adenosine or ATP binding site and a transducer domain (bridge) between the MG and adenosine binding site. The kissing aptaswitch combination described here offer an alternative design. This approach does not require any complex cloning or other expensive technique and could be extended to the development of sensor for a plethora of small molecules. Indeed we previously engineered kissing aptaswitches for adenosine and GTP [24]. They could easily be converted in light-up sensors using the approach described here. In contrast to strategies like split fluorescent protein (sFP) based sensor which require complex strategy of fluorophore maturation and binary light-up aptasensor (BLAS), our strategy is easy to execute [40–42]. However, the sensitivity of our double switch sensor remains low compared to previously described ones that made use of electrochemical, GO-based and Nanopore-based, quite sophisticated aptasensors [23,43,44]. The sensitivity of our double switch sensor could likely be improved by exploring a wider diversity of variants. We investigated here a limited number of possibilities based on rational design. We will take advantage of functional screening processes that allows to screen several millions of combinations (microfluidics, HT-SELEX, etc.) [45–47]. Indeed, such a strategy led to improved sensing properties of Mango aptamers [16].

Credit author statement

Arghya Sett: Methodology, Investigation, Writing original draft. Lorena Zara: Methodology, Investigation, Writing original draft. Eric Dausse: Investigation, Supervision. Jean-Jacques Toulmé: Conceptualization, Supervision, Funding acquisition, Writing- Reviewing and Editing.

Declaration of competing interest

The authors declare that they have no known competing financial interests or personal relationships that could have appeared to influence the work reported in this paper.

Acknowledgements

We acknowledge the support of the Agence Nationale pour la Recherche in the frame of the ERA-NET EuroNanoMed-II, (project ER-2016-2360733) and of the Conseil Régional de Nouvelle Aquitaine (grant 2017-1R30107-00013224).

Appendix A. Supplementary data

Supplementary data to this article can be found online at https://doi.org/10.1016/j.talanta.2021.122417.

References

[1] A.D. Ellington, J.W. Szostak, In vitro selection of RNA molecules that bind specific ligands, Nature 346 (1990) 818.
[2] C. Tuerk, L. Gold, Systematic evolution of ligands by exponential enrichment: RNA ligands to bacteriophage T4 DNA polymerase, Science 249 (1990) 505–510, https://doi.org/10.1126/science.2200121.
[3] S. Tombelli, M. Minunni, M. Mascini, Aptamers-based assays for diagnostics, environmental and food analysis, Biomol. Eng. 24 (2007) 191–200, https://doi.org/10.1016/j.bioeng.2007.03.003.
[4] A. Hayat, J.L. Marty, W. Mok, Y. Li, Recent progress in nucleic acid aptamer-based biosensors and Bioassays, Sensors 8 (2014) 7050–7084, https://doi.org/10.3390/s8117050.
[5] F. Pfeiffer, G. Mayer, Selection and Biosensor Application of aptamers for small molecules, Front. Chem. 4 (2016) 25, https://doi.org/10.3389/fchem.2016.00025.
[6] D. Grate, C. Wilson, Laser-mediated, site-specific inactivation of RNA transcripts, Proc. Natl. Acad. Sci. Unit. States Am. 96 (1999) 6131–6136.
[7] J.S. Paige, T. Nguyen-Duc, W. Song, S.R. Jaffrey, Fluorescence imaging of cellular metabolites with RNA, Science 335 (2012) 1194, https://doi.org/10.1126/science.1218298.
[8] E. V Dolgosheina, S.C.Y. Jeng, S.S.S. Panchapakesan, R. Cojocaru, P.S.K. Chen, P. D. Wilson, N. Hawkins, P.A. Wiggins, P.J. Unrau, RNA mango aptamer-fluorophore: a bright, high-affinity complex for RNA labeling and tracking, ACS Chem. Biol. 9 (2014) 2412–2420.
[9] F. Bouhedda, A. Autour, M. Ryckelynck, Light-up RNA aptamers and their cognate fluorogens: from their development to their applications, Int. J. Mol. Sci. 19 (2018) 44.
[10] S. Neubacher, S. Hennig, RNA Structure and cellular applications of fluorescent light-up aptamers, Angew. Chem. Int. Ed. 58 (2019) 1266–1279.
[11] J.S. Paige, K.Y. Wu, S.R. Jaffrey, RNA mimics of green fluorescent protein, Science 333 (2011) 642.
[12] R.L. Strack, W. Song, S.R. Jaffrey, Using Spinach-based sensors for fluorescence imaging of intracellular metabolites and proteins in living bacteria, Nat. Protoc. 9 (2014) 146.
[13] J. Zhang, J. Fei, B.J. Leslie, K.Y. Han, T.E. Kuhlman, T. Ha, Tandem Spinach Array for mRNA imaging in living bacterial cells, Sci. Rep. 5 (2015) 17295, https://doi.org/10.1038/srep17295.
[14] D. Guet, L.T. Burns, S. Maji, J. Boulanger, P. Hersen, S.R. Wente, J. Salamero, C. Dargemont, Combining Spinach-tagged RNA and gene localization to image gene expression in live yeast, Nat. Commun. 6 (2015) 1–10.
[15] J. Ouellet, RNA fluorescence with light-up aptamers, Front. Chem. 4 (2016) 1–12, https://doi.org/10.3389/fchem.2016.00029.
[16] A. Autour, S.C.Y. Jeng, A.D. Cawte, A. Abdolahzadeh, A. Galli, S.S. S. Panchapakesan, D. Rueda, M. Ryckelynck, P.J. Unrau, R.N.A. Fluorogenic, Mango aptamers for imaging small non-coding RNAs in mammalian cells, Nat. Commun. 9 (2018) 656.

[17] F. Bouhedda, K.T. Fam, M. Collot, A. Autour, S. Marzi, A. Klymchenko, M. Ryckelynck, A dimerization-based fluorogenic dye-aptamer module for RNA imaging in live cells, Nat. Chem. Biol. 16 (2020) 69–76.
[18] A. Sett, L. Zara, E. Dausse, J.-J. Toulmé, Engineering light-up aptamers for the detection of RNA hairpins through kissing interaction, Anal. Chem. 92 (2020) 9113–9117, https://doi.org/10.1021/acs.analchem.0c01378.
[19] S.A. Shelke, Y. Shao, A. Laski, D. Koirala, B.P. Weissman, J.R. Fuller, X. Tan, T. P. Constantin, A.S. Waggoner, M.P. Bruchez, B.A. Armitage, J.A. Piccirilli, Structural basis for activation of fluorogenic dyes by an RNA aptamer lacking a G-quadruplex motif, Nat. Commun. 9 (2018) 4542, https://doi.org/10.1038/s41467-018-06942-3.
[20] M.I. Umar, D. Ji, C.-Y. Chan, C.K. Kwok, G-Quadruplex-Based fluorescent turn-on ligands and aptamers: from development to applications, Molecules 24 (2019) 2416, https://doi.org/10.3390/molecules24132416.
[21] C. Baugh, D. Grate, C. Wilson, 2.8 Å crystal structure of the malachite green aptamer 1, J. Mol. Biol. 301 (2000) 117–128.
[22] J.R. Babendure, S.R. Adams, R.Y. Tsien, Aptamers switch on fluorescence of triphenylmethane dyes, J. Am. Chem. Soc. 125 (2003) 14716–14717.
[23] H. Wang, J. Wang, N. Sun, H. Cheng, H. Chen, R. Pei, Selection and characterization of malachite green aptamers for the development of light–up Probes, ChemistrySelect 1 (2016) 1571–1574.
[24] G. Durand, S. Lisi, C. Ravelet, E. Dausse, E. Peyrin, J.J. Toulmé, Riboswitches based on kissing complexes for the detection of small ligands, Angew. Chem. Int. Ed. 53 (2014) 6942–6945, https://doi.org/10.1002/anie.201400402.
[25] G. Durand, E. Dausse, E. Goux, E. Fiore, E. Peyrin, C. Ravelet, J.J. Toulmé, A combinatorial approach to the repertoire of RNA kissing motifs; towards multiplex detection by switching hairpin aptamers, Nucleic Acids Res. 44 (2016) 1–10, https://doi.org/10.1093/nar/gkw206.
[26] B. Chovelon, G. Durand, E. Dausse, J.-J. Toulmé, P. Faure, E. Peyrin, C. Ravelet, ELAKCA: enzyme-linked aptamer kissing complex assay as a small molecule sensing platform, Anal. Chem. 88 (2016) 2570–2575.
[27] Y. Takeuchi, M. Endo, Y. Suzuki, K. Hidaka, G. Durand, E. Dausse, J.-J. Toulmé, H. Sugiyama, Single-molecule observations of RNA–RNA kissing interactions in a DNA nanostructure, Biomater. Sci. 4 (2016) 130–135.
[28] A.M. James, M.B. Baker, G. Bao, C.D. Searles, MicroRNA detection using a double molecular Beacon approach: distinguishing between miRNA and Pre-miRNA, Theranostics 7 (2017) 634–646, https://doi.org/10.7150/thno.16840.
[29] R.D. Jenison, S.C. Gill, A. Pardi, B. Polisky, High-resolution molecular discrimination by RNA, Science 263 (1994) 1425–1429.
[30] A. Wrist, W. Sun, R.M. Summers, The theophylline aptamer: 25 Years as an important tool in cellular engineering Research, ACS Synth. Biol. 9 (2020) 682–697, https://doi.org/10.1021/acssynbio.9b00475.
[31] Q. Pu, S. Zhou, X. Huang, Y. Yuan, F. Du, J. Dong, G. Chen, X. Cui, Z. Tang, Intracellular selection of theophylline-sensitive Hammerhead Aptazyme, Mol. Ther. Nucleic Acids 20 (2020) 400–408, https://doi.org/10.1016/j.omtn.2020.03.001.
[32] G.R. Zimmermann, R.D. Jenison, C.L. Wick, J.-P. Simorre, A. Pardi, Interlocking structural motifs mediate molecular discrimination by a theophylline-binding RNA, Nat. Struct. Biol. 4 (1997) 644–649.
[33] G.R. Zimmermann, C.L. Wick, T.P. Shields, R.D. Jenison, A. Pardi, Molecular interactions and metal binding in the theophylline-binding core of an RNA aptamer, RNA 6 (2000) 659–667.
[34] C. Boiziau, E. Dausse, L. Yurchenko, J.-J. Toulmé, DNA Aptamers selected against the HIV-1 trans-activation-responsive RNA element form RNA-DNA kissing complexes, J. Biol. Chem. 274 (1999) 12730–12737.
[35] F. Ducongé, J.-J. Toulmé, In vitro selection identifies key determinants for loop–loop interactions: RNA aptamers selective for the TAR RNA element of HIV-1, RNA 5 (1999) 1605–1614.
[36] F. Ducongé, C. Di Primo, J.J. Toulmé, Is a closing "GA pair" a rule for stable loop-loop RNA complexes? J. Biol. Chem. 275 (2000) 21287–21294, https://doi.org/10.1074/jbc.M002694200.
[37] S. Cao, S.-J. Chen, Structure and stability of RNA/RNA kissing complex: with application to HIV dimerization initiation signal, RNA 17 (2011) 2130–2143.
[38] M.N. Stojanovic, D.M. Kolpashchikov, Modular aptameric sensors, J. Am. Chem. Soc. 126 (2004) 9266–9270.
[39] W. Xu, Y. Lu, Label-free fluorescent aptamer sensor based on regulation of malachite green fluorescence, Anal. Chem. 82 (2009) 574–578.
[40] K.K. Alam, K.D. Tawiah, M.F. Lichte, D. Porciani, D.H. Burke, A fluorescent split aptamer for visualizing RNA–RNA assembly in Vivo, ACS Synth. Biol. 6 (2017) 1710–1721, https://doi.org/10.1021/acssynbio.7b00059.
[41] M. Debiais, A. Lelievre, M. Smietana, S. Müller, Splitting aptamers and nucleic acid enzymes for the development of advanced biosensors, Nucleic Acids Res. 48 (2020) 3400–3422, https://doi.org/10.1093/nar/gkaa132.
[42] D.M. Kolpashchikov, A. Spelkov, Binary (split) light-up aptameric sensors, Angew. Chem. Int. Ed. 60 (2021) 4988–4999.
[43] L. Feng, Y. Chen, J. Ren, X. Qu, A graphene functionalized electrochemical aptasensor for selective label-free detection of cancer cells, Biomaterials 32 (2011) 2930–2937.
[44] L. Zhu, R. Zhao, K. Wang, H. Xiang, Z. Shang, W. Sun, Electrochemical Behaviors of Methylene blue on DNA modified Electrode and its application to the detection of PCR Product from NOS sequence, Sensors 8 (2008) 5649–5660, https://doi.org/10.3390/s8095649.
[45] A. Autour, F. Bouhedda, R. Cubi, M. Ryckelynck, Optimization of fluorogenic RNA-based biosensors using droplet-based microfluidic ultrahigh-throughput screening, Methods 161 (2019) 46–53.
[46] P. Dao, J. Hoinka, M. Takahashi, J. Zhou, M. Ho, Y. Wang, F. Costa, J.J. Rossi, R. Backofen, J. Burnett, T.M. Przytycka, AptaTRACE Elucidates RNA sequence-structure motifs from selection Trends in HT-SELEX Experiments, Cell Syst 3 (2016) 62–70, https://doi.org/10.1016/j.cels.2016.07.003.
[47] A. Sinha, P. Gopinathan, Y.-D. Chung, H.-Y. Lin, K.-H. Li, H.-P. Ma, P.-C. Huang, S.-C. Shiesh, G.-B. Lee, An integrated microfluidic platform to perform uninterrupted SELEX cycles to screen affinity reagents specific to cardiovascular biomarkers, Biosens. Bioelectron. 122 (2018) 104–112.